Study of Liquid Metal Embrittlement of steels by EBSD

July 12-17, 2009 Ottawa, Ontario, Canada

T.Auger[1,a], L.Medina-Almazan[b], C.Rey[a], P.Bompard[a], D.Gorse[c]

a MSSMAT-ECP, UMR CNRS 8579, Grande voie des vignes, 92290 Chatenay-Malabry, France, b Departamento de Tecnología de Materiales, Instituto Nacional de Investigaciones Nucleares, Carretera México-Toluca s/n, La Marquesa, Ocoyoacac*, C.P. 52750, Mexico, c LSI, UMR CNRS 7642, Ecole Polytechnique, Palaiseau, France*

1-Introduction

Liquid metal embrittlement (LME) of steels is of renewed interest in the framework of nuclear reactors and spallation neutron sources projects using liquid metals as coolant. The structural materials for these systems are selected according to their resistance to liquid metal corrosion, irradiation embrittlement and compatibility with the coolant. These stringent constraints leave two classes of materials, austenitic steels and martensitic/ferritic steels. The reference materials for these systems are the 316L austenitic steel and the T91 martensitic steel, a modified 9Cr1Mo alloy. LME of these materials in contact with mercury (Hg) and (PbBi) has been demonstrated in various works [1,2]. The fracture mode proceeds either by cleavage or by shear cracking depending upon the geometry and the mechanical solicitation (mode I or mixed mode II/III). A fracture mechanics approach (J-δa) has been developed in plane stress with thin sheets allowing to a good approximation a measurement of the crack length by optical means. Indeed one of the difficulties of fracture mechanics with a liquid metal environnement is the fact that the medium is opaque and conductive. This adaptation of fracture mechanics reduces the propagation problem to a quasi-2D problem. It showed that the liquid metal reduces the energy required for crack extension by 30 to 50% supporting the case for LME [3]. The mechanism of LME in general is still a matter of debate and it is the purpose of this paper to report a study of cracking induced by a liquid metal by Electron Back Scattering Diffraction (EBSD).

2- Experimental
2-1 materials

The martensitic steel T91 and the austenitic stainless steel 316L were delivered as hot rolled and heat treated plates with a thickness of 15 mm by Industeel, Arcelor group. The chemical composition is reported below (Table 1). They have been used in the metallurgical standard conditions, solution annealed at 1050-1100°C for 316L; normalizing at 1050°C during 1 minute per millimeter,

---

[1] E-mail: *thierry.auger@ecp.fr*
Tel : 33 (0) 1 41 13 15 97

thus 15 minutes, cooling with water to room temperature plus tempering at 770°C, holding for three minutes par millimeter of thickness, thus 45 minutes and then air cooling in still air to room temperature. The 316L steel under consideration has an average grain size of 24 μm; for the T91 steel, the average prior austenite grain size is 20 μm.

Table1. Composition of 316L and T91 steels used in the present work.

Steel	C	Si	Mn	P	S	Cr	Mo	Ni	Al	Cu	Nb	V
316L	0.0185	0.67	1.81	0.032	0.0035	16.73	2.05	9.97	0.0183	0.23	-	0.07
T91	0.1025	0.22	0.38	0.021	0.0004	8.99	0.89	0.11	0.0146	0.06	0.06	0.21

2-2 Specimen preparation

Both CCT (Center Crack Tension) and CT (Compact-Tension) geometries have been used in this work. In both geometries the notch is used as mercury reservoir. The side-grooved CT geometry is used in order to produce an enhanced triaxiality (Figure 1b). Two groove radii for the CT specimen were used (R4 and R6). The CCT specimen have 1 to 2mm thickness.
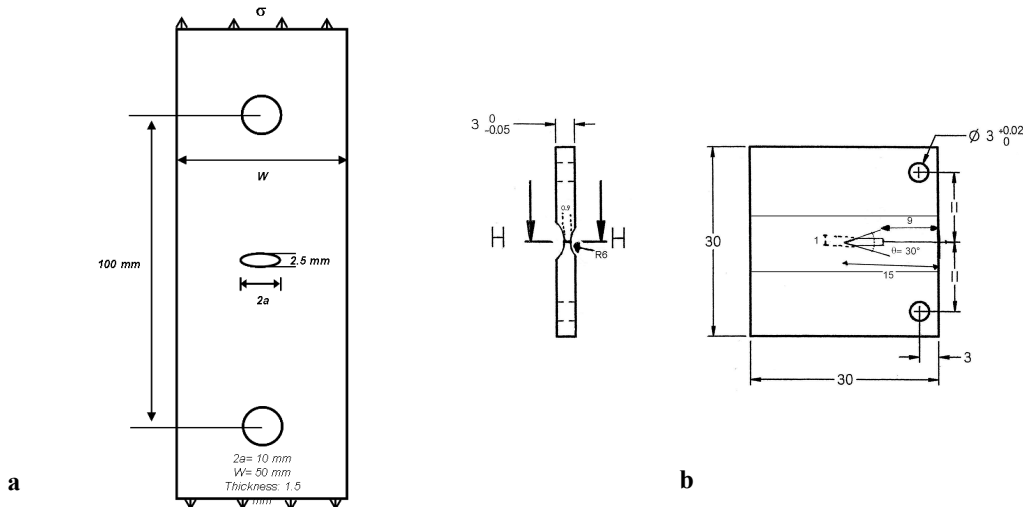
Figure 1. Geometry of CCT (a) and CT (b) specimens used in this work.

Wetting of 316L and T91 steels by mercury is hindered by their native oxide. Because the chemical nature of the native oxide depends on the steel alloying elements (High Chromium content of 316L steel) we have developped two procedures to obtain wetting by mercury of 316L and T91 steels [4].

For both steels, the specimen surface is diamond polished (down to 1μm) and the inner part of the notch walls are carefully mechanically polished using SiC papers to grade 4000 (diamond polishing being too impractical in this confined space). The specimens are then ultrasonically cleaned in absolute ethanol and dried in air. This specimen preparation does not avoid the formation of a native oxide film growing at the specimen surface and on the notch walls, but may possibly limits its barrier role.

For 316L steel, mechanical polishing is followed by chemical etching using a 4% HCl aqueous solution [4]. It allows for an efficient wetting of the notch and bared crack walls by mercury which progressively replaces the acidic solution at the steel crack walls and spreads spontaneously. After usually 120 minutes, the notch tip is completely wetted. Samples are then withdrawn from the acidic solution and carefully cleaned to remove any solution traces.

For T91 steel, after mechanical polishing, the notches are immediately filled with a mercury drop using a syringe. The mercury is pressed to force the contact with the notch walls and left for ageing. After 48h, notch walls are usually wetted by mercury and the specimen is ready for test.

2-2 Mechanical testing, fracture mode and EBSD preparation

Mechanical test have been performed on a MTS 20/MH electromechanical tensile machine. The specimens are loaded at constant cross head speed (Figure 2). The fracture initiation proceeds by cleavage.
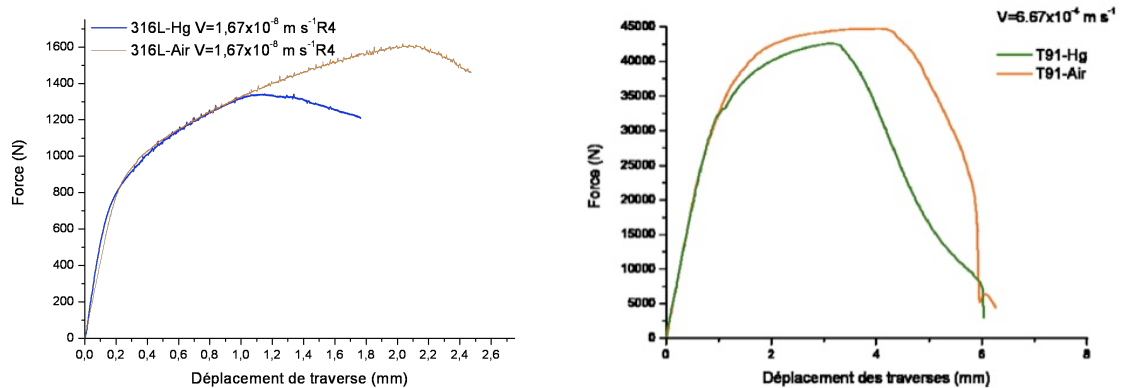
Figure 2 : Load/displacement reference curves and in contact with Hg curves for 316L (Left) with the R4 CT geometry and T91 (Right) in the CCT geometry

The crack propagation in our geometry is found to proceed by shear cracking (Figure 3a and 3b). This fracture mode seems to be induced by the plane stress mechanical loading state that favors 45° transverse shear plastic deformation. The same shear cracking mode is seen with the austenitic steel as with the martensitic steel. One of the most striking observation is that no microstructural feature can be seen on the fracture surface pointing to a very localized dislocation/surface interaction problem (Figure 3b).

In order to nucleate a crack for analysis by EBSD, CT specimens of 316L and T91 steels have been loaded in air and in mercury at 1.67×10^{-8} m.s^{-1}. The test is stopped when the maximal load falls by 10% from its maximum. The sample is then dismounted and a disc is extracted from the notch tip zone by spark erosion. The sample is coated by a conductor resin and mechanically polished in order to remove the roughened surface produced by plastic deformation. Electropolishing is performed again followed by ion beam sputtering. This allowed for an analysis of the crack tip along the plane A (Figure 3a). The CCT specimens in 316L and T91 steels were tested until complete fracture. Mercury was removed by

ultrasonic exposure in water. This allowed an EBSD analysis of the area close to the fracture surface corresponding to a cut along plane B.
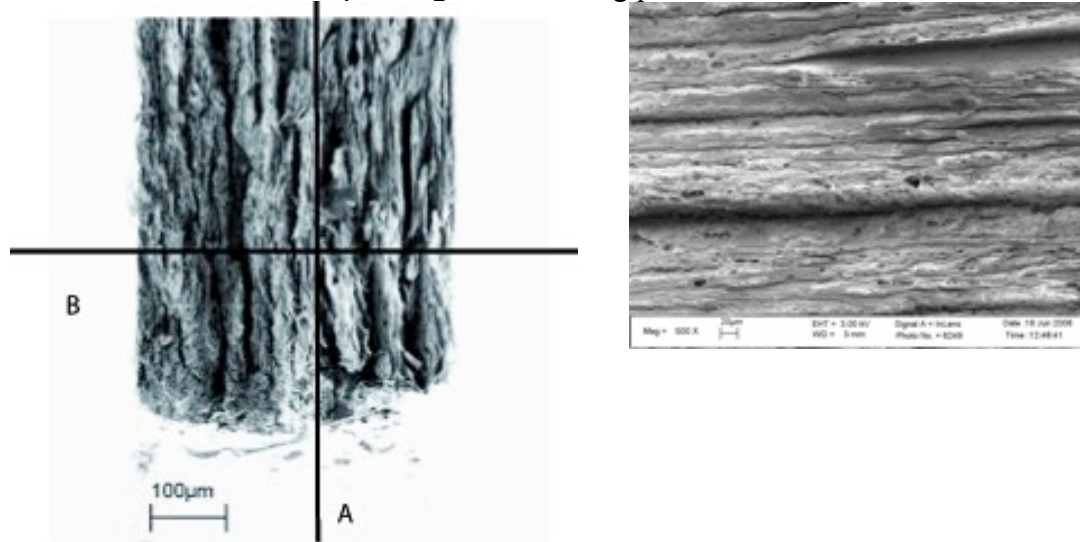
Figure 3 : Left) Fracture surface on a CT specimen (vertical crack propagation) and Right) Fracture surface of 316L CCT specimen (horizontal crack propagation)

4- EBSD analysis
4-1 316L-Hg

EBSD mapping has been performed on a control CT specimen before mechanical tests : 316L steel has no preferential grain orientation (figure 4a). After mechanical testing, a disc is extracted from the notch tip zone by spark erosion. An EBSD pattern map was obtained along the crack path (Figure 4b). That was not the case of the specimen tested in air (fig. 4c). For this last specimen, it was only possible to obtain EBSD patterns of the less deformed grains, which are the less well- oriented grains to glide, located far ahead of the crack tip zone. The remarkable feature is that the overall plastic deformation is reduced upon cracking compared to cracking in air, consistent with the fracture mechanics assessment of a reduced energy spent for crack extension.
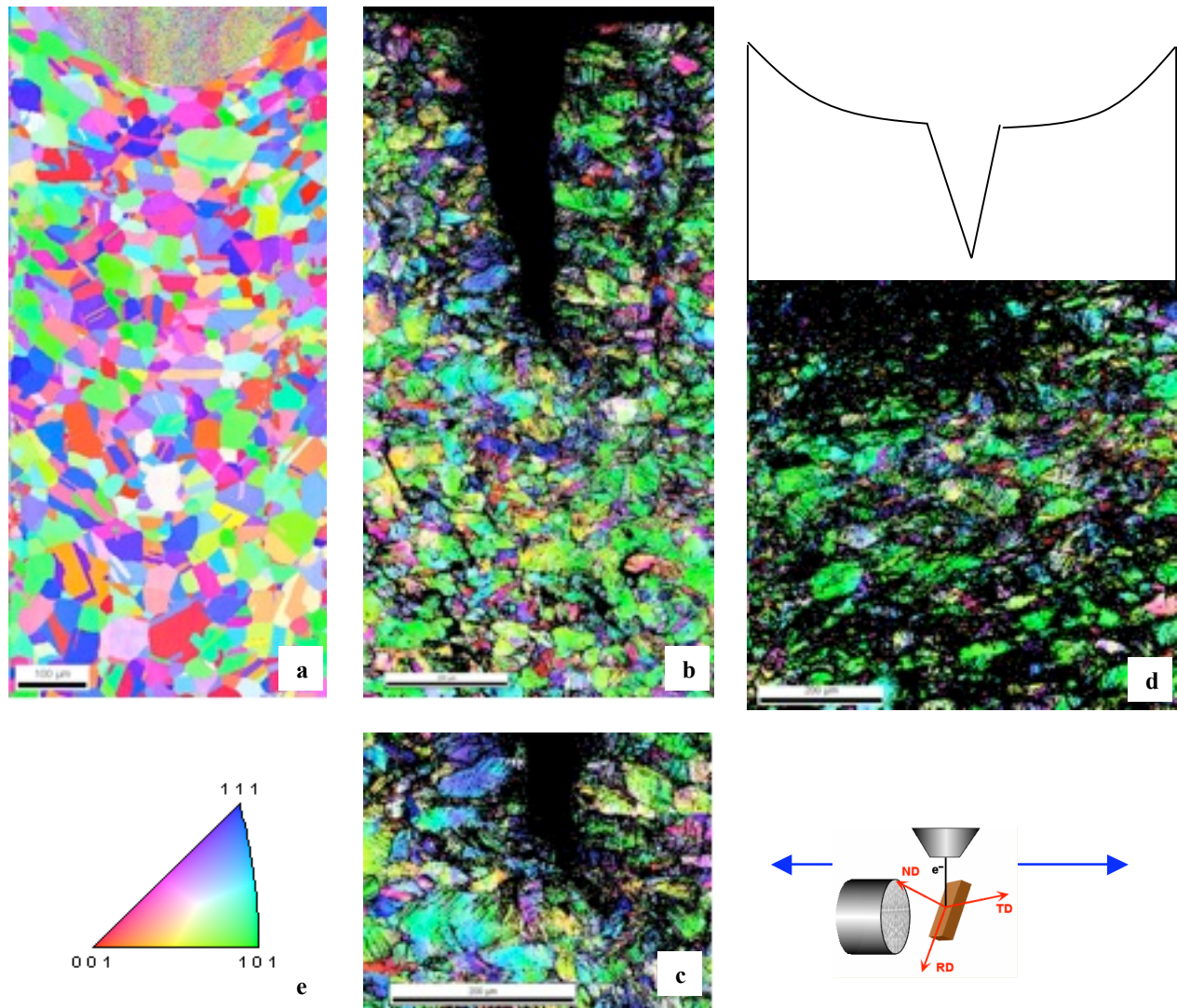
Figure 4. EBSD mappings (image quality map + hkl) of CT specimens in 316L steel. a) Before mechanical test; b) mechanical test in contact with mercury; c) detail of (b) at the crack tip zone; d) mechanical test in air; e) legend for crystal orientation.

The normal ductile crack propagation is actually impossible to analyze by EBSD due to the high level of plastic deformation involved. The quality pattern of the EBSD mapping decreases in general with the stored density of dislocations up to a threshold where it prevents correct indexing.

The EBSD mapping of the plane B cut in an area close to the fracture surface is shown in figure 5. One can notice in the transverse cut that the angle at the top of a vein is close to 60°. The EBSD mapping shows also very little desorientation inside the grains very close to the surface (EBSD step size of 0.1µm). The grains have rotated to allow for shear. Cracking is very likely to have occurred in crystallographic planes after grains rotation. One can make the hypothesis that cracking occurs in {111} family glide plane promoted by an intense plastic deformation localization. This conclusion seems to be valid on a mesoscopic scale. However, it was not possible to reliably index the crystallographic

orientation close to the fracture surface in this case due to experimental artifacts near the edges.
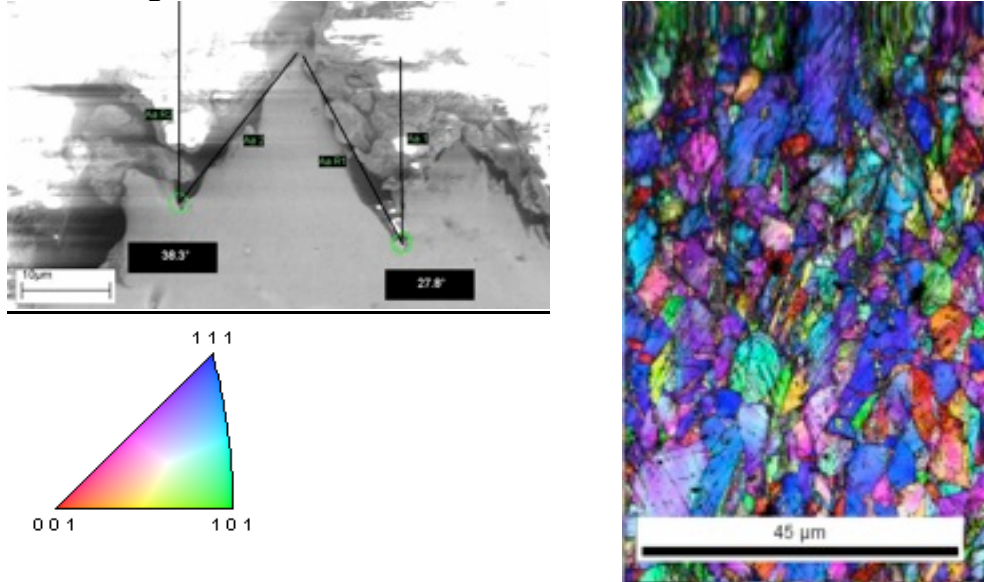
Figure 5 : a) viewgraph of the transverse cut on CCT 316L specimen b) EBSD mapping in the ND direction

4-2 T91-Hg

Due to the finer microstructure of the T91 steel, the EBSD step size was always set to 0.1 μm. The EBSD analysis was performed around the crack tip corresponding to a crack propagated in the CT specimen by roughly 1mm. The EBSD analysis qualitatively shows that in contact with Hg the martensitic steel is comparatively less deformed than the one in contact with air (Figure 6a, 6b & 6c). Contrary to the 316L case, it is possible to correctly index (i.e. with a good quality index) the crystallographic orientation around the crack tip almost up to the edges of the crack (Figure 6d). It is to be noted as well that a very clear sub-grain structure is formed during the deformation process in both cases (316L and T91 in contact with Hg). Liquid metal induced cracking seems to restrict plastic deformation to a smaller number of glide systems.
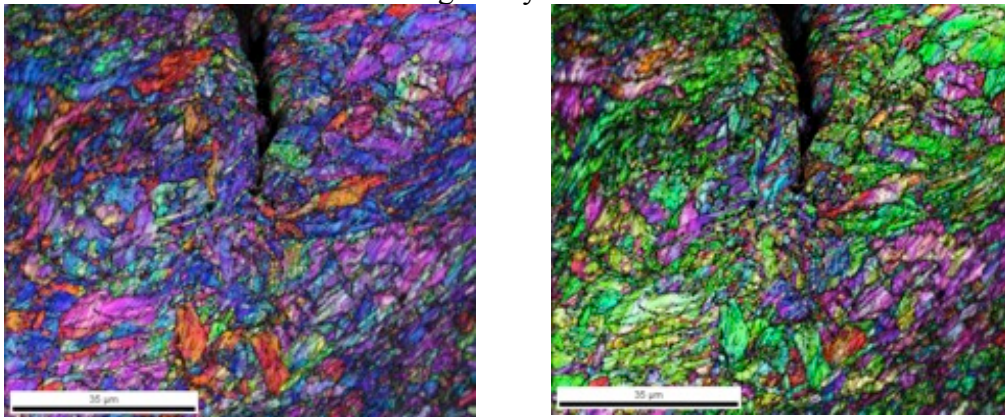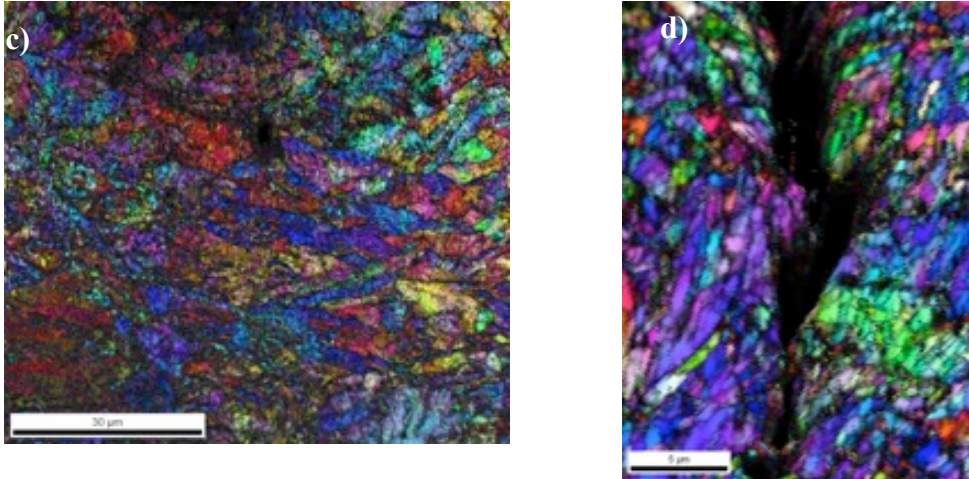
Figure 6: a) EBSD mapping in the ND direction for T91-Hg b) EBSD mapping in the TD direction for T91-Hg c) EBSD mapping in the ND direction for T91 (quality factor superposed) d) Zoom over the crack tip for T91 in contact with Hg

Given the preferential orientation found in the EBSD mapping around the crack tip and the orientation of the sample with the macroscopic stress, it is found in the case of this bcc alloy that cracking seems to occur along the {110} family glide planes. Here again, it would be promoted by an intense strain localization at the crack tip.

5- Discussion

The embrittlement of the 316L austenitic steel and the martensitic T91 steel has been studied by a fracture mechanics setup and the energy required to extend the cracks is clearly reduced by the presence of a liquid metal at the crack tip [3]. It is clear therefore that we deal in this work with an embrittlement effect induced by the liquid metal taking place at room temperature. The fracture mode by shear cracking is believed to be due to the plane stress mechanical loading state experienced by the specimens. On the other hand, the amount of plastic deformation required before brittle cracking is large and could cast a priori doubts about the possibility to use EBSD mapping to study the phenomenon. The first interesting result of this work is the fact that EBSD reveals itself as a very powerful tool to study LME as the reduction in ductility allows for a better index patterning. Another interesting point, in line with the fracture mechanics assessment [3], is that the plastic deformation in a CT or CTT geometry is reduced ahead of the crack tip when cracking occurs by LME. This was also reflected in a Crack Tip Opening Analysis of the crack propagation. Instead, with the standard fracture mode by ductile void growth and coalescence, the amount of plastic deformation prevents in general a useful EBSD analysis with these materials.

The cracking mechanism seems to occur in a two steps phase: first the grains rotate during plastic deformation to accommodate the plane stress condition and the 45° macroscopic shear constraint. Then cracking would occur,

at least at the mesoscopic scale, in crystallographic glide planes: for fcc alloys in the {111} family glide planes and for bcc alloys in the {110} family glide plane. The fracture surface then would be a mixture of crystallographic fracture controlled by the macroscopic constraints and this would give the characteristic vein pattern (Figure 7). This would go along with the common view of LME being a process of cracking due to the lowering by the liquid metal of the surface energy, the rehbinder effect.
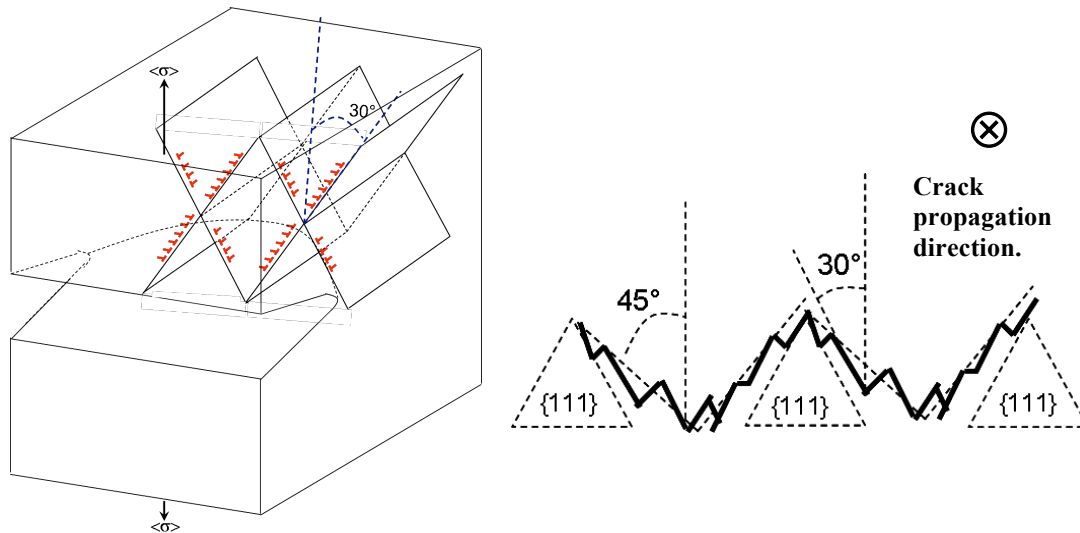
Figure 7: Left) schematic of the crack tip and the activated glide planes. Right) a cross section of the resulting fracture surface with a crystallographic fracture path.

The atomistic scale mechanism is beyond the scope of the EBSD technique. There seems to exist some threshold required to trigger crack propagation that would need to be investigated by other techniques. The mechanism could very well be a variant of the Lynch mechanism of dislocation emission at the crack tip induced by the liquid metal [5]. While this is certainly a key component for any embrittlement scenario able to describe our results, it also requires a detailed account of how the enhanced plasticity interacts with cracking. It also hardly accounts for a cleavage type fracture and certainly cannot be a universal mechanism. It is also felt that the EBSD technique would be very well suited to give guidelines for the implementation of a description of LME into a crystalline plasticity modeling approach.

References:
[1] L.Medina-Almazan, T.Auger, D.Gorse, J. Nuc. Mater. 376 (2008) 312-316
[2] Z.Hamouche-Hadjem, T.Auger, I.Guillot, D.Gorse, J. Nuc. Mater. 376 (2008) 317-321
[3] T.Auger, Z. Hamouche, L. Medina-Almazàn, D. Gorse, J. Nuc. Mater. 377 (2008) 253-260
[4] L. Medina-Almazán, J.-C. Rouchaud, T. Auger, D. Gorse, J. Nuc. Mater. *375 (2008) 102-112*
[5] S.P.Lynch, Acta Metall. 36 (1988) 2639-2661